DOI:
10.1109/LRA.2020.2976303

Document Version
Peer reviewed version

Creating a Soft Tactile Skin employing Fluorescence based Optical Sensing

Federica De Chiara[1,*], Shuxin Wang[2], and Hongbin Liu[1]

***Abstract*—Currently, optical tactile sensors propose solutions to measure contact forces at the tip of flexible medical instruments. However, the sensing capability of normal pressures applied to the surface along the tool body is still an open challenge. To deal with this challenge, this paper proposes a sensor design employing an angled tip optical fiber to measure the intensity modulation of a fluorescence signal proportional to the applied force. The fiber is used as both emitter of the excitation light and receiver of the fluorescence signal. This configuration allows to (i) halve the number of optical fibers and (ii) improve the signal to noise ratio thanks to the wavelength shift between excitation and fluorescence emission. The proposed design makes use of soft and flexible materials only, avoiding the size constraints given by rigid optical components and facilitating further miniaturization. The employed materials are bio-compatible and guarantee chemical inertness and non-toxicity for medical uses. In this work, the sensing principle is validated using a single optical fiber. Then, a soft stretchable skin pad, containing four tactile sensing elements, is presented to demonstrate the feasibility of this new force sensor design.**

***Index Terms*—Soft Robot Materials and Design, Force and Tactile Sensing, Soft Sensors and Actuators, Soft Robot Applications, Medical Robots and Systems**

I. INTRODUCTION

TACTILE sensing allows robotic devices to work efficiently in constrained environments [1]. In minimally invasive surgery (MIS), where the environment is unstructured and space-limited, flexible robotic arms equipped with tactile sensors can significantly improve the perception of the applied force by the physician during surgical or diagnostic interventions. This would prevent the application of excessive pressures with consequent damage or perforation of internal tissues. For this reasons such devices have been increasingly attracting interest worldwide [2]–[4].

During its navigation within the human body the flexible instrument typically applies, to blood vessels or internal organs, pressure and shear forces by two points: its tip and the external surface of its main frame [5]. In order to provide the sense of touch while using flexible MIS tools, numerous methods have been adopted such as piezoresistive or capacitive materials and strain gauges or conductive elastomers where the applied force is measured based on the electrical signals [6]–[9]. Magnetic tactile sensors have also been employed to measure applied forces from changes in the magnetic field [10]–[13]. The main drawback of the above sensing principles is that they are susceptible to electromagnetic disturbance effects in the environment.

Optical tactile sensing can effectively address the above limitations and presents advantages in miniaturization, therefore it has been successfully applied in clinical practices [14]–[16]. Optical based tactile sensing makes use of optical fibers and measure forces by observing changes in the properties of the optical signal carried within the fiber [21]. The probed optical signal properties can be intensity [17], phase [18], frequency [19], or polarization [20]. To date, the optical tactile sensing technology provides adequate solutions for tool tip force sensing. However how to apply this technology to add force sensing capability along the flexible body of the instrument is still an open challenge in the field. The design proposed to overcome such challenge is a fluorescence signal based pressure sensor employing an angled tip optical fiber.

Fluorescent dyes are substances able to absorb light with a certain wavelength and emit light with a longer wavelength known as fluorescence emission. Thus, having different wavelengths, absorption light and fluorescence emission can be distinguished from each other within the same optical fiber that can be used as both emitter and receiver avoiding the need of optical couplers or bifurcated bundles. Such fiber, equipped with an angled tip, can be placed in parallel with the axis of a medical tool shaft. This configuration (fig. 1c) minimises the thickness of the soft skin applied to the external surface of the tool by halving the number of fibers. Furthermore, an angled tip optical fiber allows the detection of normal pressures applied on the tool body without the use of rigid components such as mirrors [22]–[24]. These characteristics can facilitate the fabrication of an extended design with a cylindrical shell shape which can be adapted to the external surface of non-planar medical tools, creating a kind of flexible covering skin doped with fluorescent dyes (fig. 1e).

In the case of multiple fibers embedded into the soft material composing the skin, each fiber works like a tactile sensing element. The combination of multiple sensing elements can provide not only information about the

This work was supported by the National Natural Science Foundation of China (NSFC) No.51520105006 and the EPSRC, Grant No.: EP/R013977/1.

[1]Federica De Chiara and Hongbin Liu are with School of Biomedical Engineering, King's College London, London, United Kingdom.
*Corresponding author. Federica.De_Chiara@kcl.ac.uk Hongbin.Liu@kcl.ac.uk
[2]Shuxin Wang is with School of Mechanical Engineering, Tianjin University, Tianjin, China.

The authors would like to thank Dr Frederic Festy for the original idea of using fluorescence based optical sensing for tip contact force sensing.

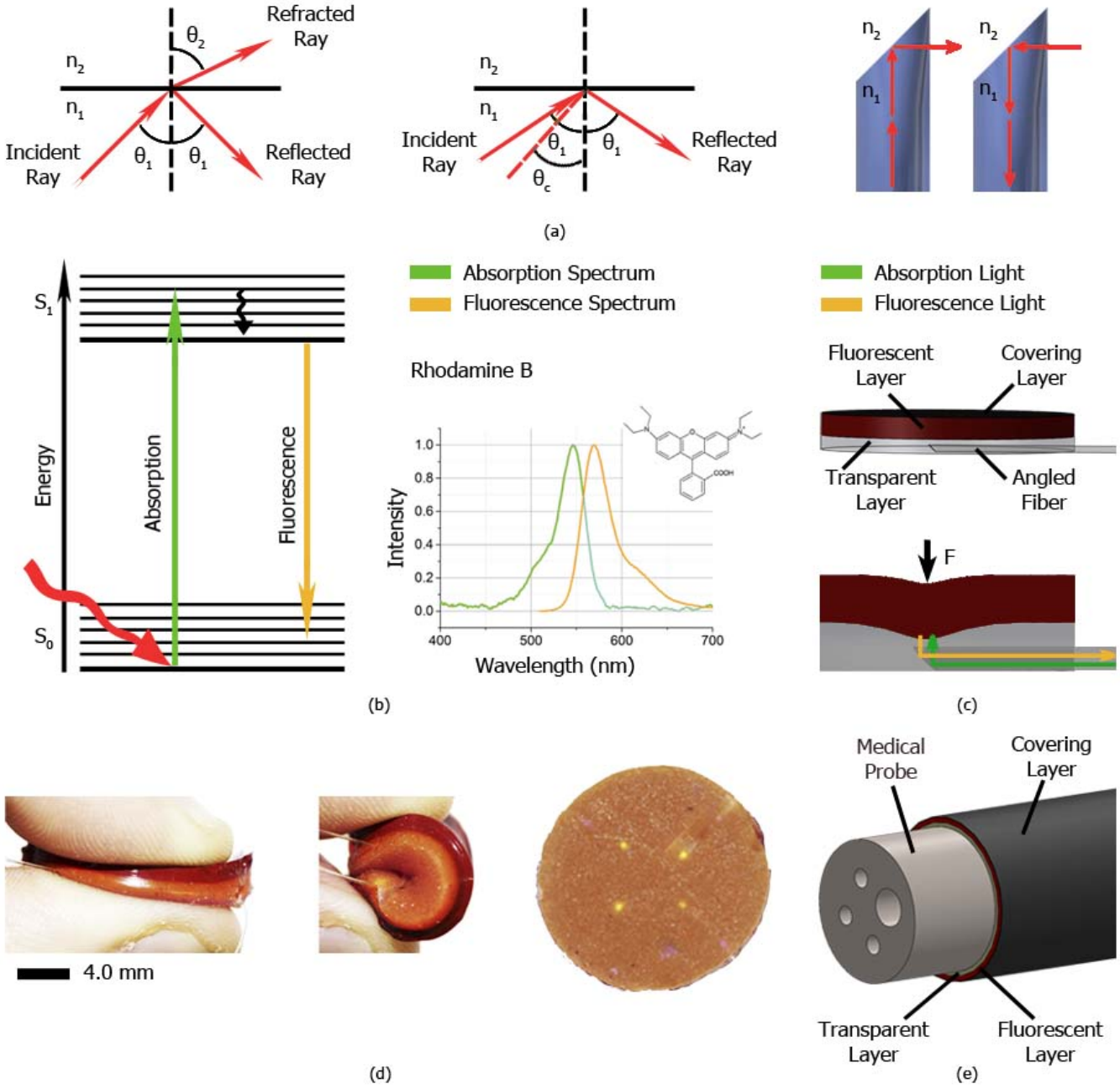

Fig. 1: **Stretchable tactile array sensor based on fluorescence. (a)** Light passing through two transparent media with different refractive indices is partially reflected into the first medium and partially transmitted through the second medium. When the incidence angle is higher than the critical angle, Total Internal Reflection (TIR) occurs (readapted from [25]). This principle can be applied to optical fibers, where the tip is cut at an angle higher than the critical angle. **(b)** Light with a specific wavelength can be absorbed causing an electron of a molecule or an atom to leave the ground state and reach a higher energy level. Fluorescence occurs when the electron relaxes again to its ground state by releasing energy in the form of visible light. Absorption and emission spectra of Rhodamine B are presented (readapted from [26]). **(c)** The proposed sensor is characterized by a layer structure of soft material. The optical fiber is embedded into the lower transparent layer. Its angled tip implements the TIR principle: the light of the light source (green arrow) reaches the fluorescent layer and the fluorescence emission (yellow arrow) is transmitted by the fiber to the imaging system. When a force is applied to the sensor, the lower surface of the fluorescent layer gets closer to the fiber and a higher light intensity can be detected by the camera. **(d)** Multiple optical fibers can be placed into the transparent silicone layer, leading to manufacture a tactile array sensor. The sensor is flexible and can be bent to a small radius of curvature. **(e)** The proposed sensor can be applied to the external surface of medical tool shafts, such as the one of an endoscope.

magnitude of the applied pressure, but also about the position of its application point. Moreover, biocompatible fluorescent dyes can be adopted to guarantee chemical inertness and nontoxicity.

The sensing principle was first validated using a single optical fiber. Than a soft and stretchable skin pad, containing four tactile sensing elements, was made as feasibility study for the application of this design to the flexible body of medical instruments. The case study, took as model of the presented sensor, is the measure of pressures applied to the external surface of a catheter during endoscopic interventions.

II. SENSING CONCEPTS

A. Total Internal Reflection and Prismatic-Tip Optical Fiber

Light passing through an interface between two different media may be partially reflected and partially transmitted through the second medium. This phenomenon is described by the well known *Snell's law*:

$$n_1 sin(\theta_1) = n_2 sin(\theta_2)$$

where n_1 and n_2 are the indices of refraction of the two media, θ_1 angle of incidence and θ_2 angle of refraction.
In the specific case of $n_1 > n_2$, θ_2 can reach its limit value of $90°$, corresponding to the condition $\theta_1 = \theta_c$ where θ_c is called *critical angle* and is defined as follows:

$$\theta_c = \arcsin(\frac{n_2}{n_1})$$

For values of $\theta_1 > \theta_c$, refraction does not occur anymore and the light is totally reflected into the first medium. This phenomenon is known as *total internal reflection* (*TIR*).
An optical fiber works with the same principle. If the core of a fiber has a refractive index n_1 higher than the refractive index of the air n_2 and the tip of the optical fiber is cut with an angle equal or higher than the critical angle, then total internal reflection occurs. The core of the fiber used is made of acrylic polymer PMMA (polymethylmethacrylate) and its refractive index is 1.492. Then the critical angle for the considered fiber is around $42°$. To fulfil TIR requirements we can therefore cut the tip at $45°$. Thus, the light transmitted by the fiber is reflected at $90°$ and it can get out. Similarly, light coming from outside can be reflected at $90°$ by the $45°$ cut surface and then it can be transmitted through the fiber (fig. 1a). For this reason a prismatic tip fiber will be able to receive light signals at normal incidence with respect to its optical axis without the use of rigid optics. This allows the fiber to run parallel and close to the surface of a flexible tool such as an endoscope, making it easily adaptable to non-planar surfaces.

B. Physical Principles of Fluorescence

When a photon reaches a material surface it may cede its energy to an electron. If such energy is higher than the energy gap between the initial atomic level of the electron and an adjacent higher one, the electron is promoted to the higher level. The lower energy atomic level is now empty. Such vacancy can be filled with an electron decaying from a higher energy level by the emission of a photon. If this is the case, such photon can be seen as visible light and we call it *fluorescence*. The average time lapse τ between the excitation event and the return to the ground state by the fluorescence emission is the fluorophore lifetime [27]. The lifetime is usually in the order of magnitude of $10ns$.
Fluorescence light is emitted at longer wavelength than the excitation signal. This phenomenon, known as *Stokes shift*, is mainly due to non-radiative relaxation to the lowest

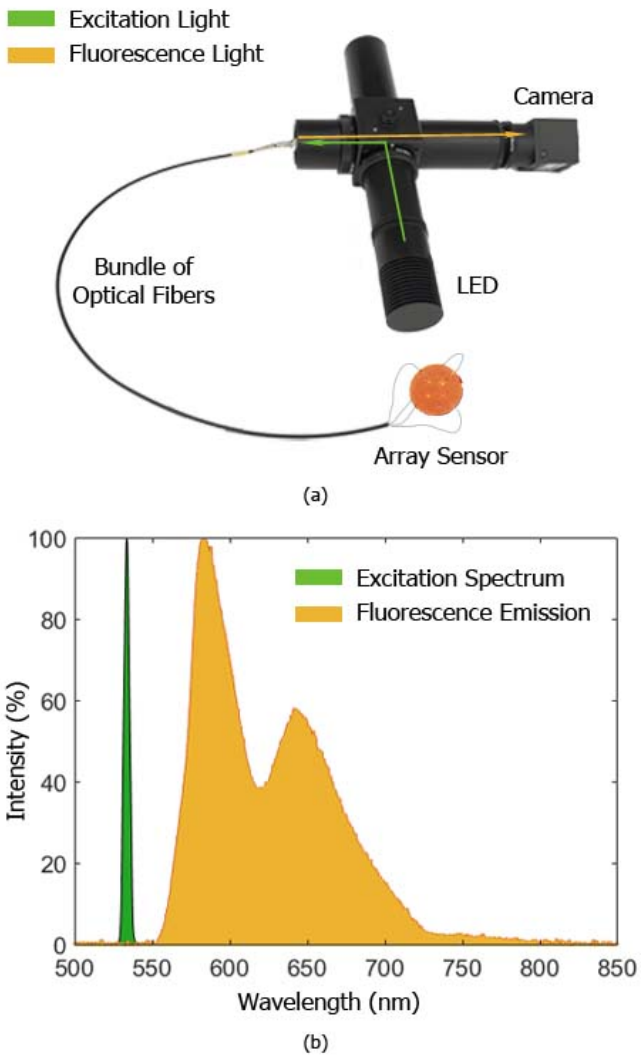

Fig. 2: **Experimental setup and acquired spectra. (a)** The array sensor is connected to the fluorescence imaging system using a bundle of angled tip optical fibers. The light emitted by the LED reaches the sensor which consequently emits fluorescence light. **(b)** As a result of the applied filtering system, the spectra of the excitation light source and fluorescence emission cover different wavelength ranges. Thus, the camera of the imaging system is able to detect the fluorescence signal filtering out the light source completely.

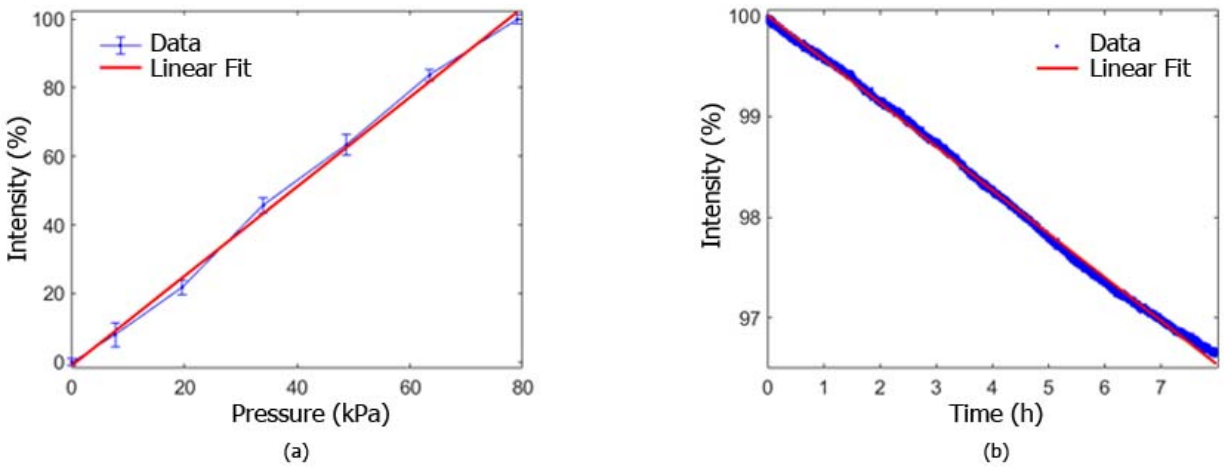

Fig. 3: **Experimental evaluation. (a)** Calibration curve: 30 measurements for each point were acquired to carry out the repeatability experiment. **(b)** Measure of photobleaching: the slope of the intensity decay over 8 hours was measured 3 times, giving values within the same order of magnitude.

vibrational energy level of the excited state, in which the excitation energy is dissipated as heat (black wavy arrow in fig. 1a).
Thanks to this clear distiction between excitation and signal wavelength, fluorescence has been extensively used in biochemical and medical applications where the signal to noise ratio is particularly critical [28]. The specific fluorescent dye used in this work is Rhodamine B and its absorption and emission spectra are presented in fig. 1b.

C. Physical Design of the Sensor and Working Principle

The sensor has a round shape with diameter of $11.50mm$ and it is characterized by three layers: the first one is a transparent silicone layer (thickness of $2mm$), the second one is a silicone mixture containing the fluorescent dye (thickness of $2mm$) and finally a black paint was sprayed as third layer to prevent environmental light from interfering with the sensor.
The fluorescent dye (Rhodamine B, Sigma-Aldrich, excitation wavelength $550nm$, fluorescence wavelength $570nm$) was diluted in methanol with 1:10 weight ratio. Then, the solution was mixed with clear silicone (Sorta-Clear^{TM} 12, Bentley Advanced Materials) with 1:10 weight ratio.
A $1mm$ optical fiber was cut and polished to get an angled tip emitting and receiving light at once, based on the total internal reflection (TIR) principle. A mold was designed to keep the fiber in place during the silicone curing process. As result, the fiber is fixed inside the transparent layer, at the distance of about $1mm$ from the fluorescent layer.
The fluorescent layer absorbs light transmitted by the fiber and emits, in turn, light with a longer wavelength as a result of fluorescence. When a force is applied on the sensor the fluorescent layer is deformed and the distance between fiber and fluorescent surface decreases. As a result, the light emitted by the fiber reaches the fluorescent layer with a higher intensity. Consequently also the fluorescence excitation increases, enhancing eventually the fluorescence emission (fig. 1c).

III. IMAGING SYSTEM

The imaging system is presented in fig. 2a. The excitation light emitted by the LED is reflected at 90° and then reaches the fiber (green arrow). Once the LED light illuminates the sensor, fluorescence is emitted by the dopped silicone layer and transmitted back to the camera through the fiber (yellow arrow).
The employed camera is Blackfly USB3, $2.3MP$, $41fps$. The excitation spectrum is nominally centered at $530nm$ (green) with a full width at half maximum (FWHM) of $4.5nm$ while the fluorescence spectrum stretches from $555nm$ to $800nm$ (yellow-red). Excitation and emission spectra are shown in fig. 2b.
To improve the signal to noise ratio the system is equipped with an optical band pass filter matching the fluorescence emission of Rhodamine B.

IV. EVALUATION EXPERIMENTS

Evaluation experiments were carried out using the sensor design as described previously. One end of the optical fiber was embedded into the sensor; while the other end was connected to the imaging system to detect the fluorescence light and its intensity variation when a force is applied.
A 6-axes force/torque sensor (ATI Nano-17, resolution $0.003N$) was mounted on a motorized linear guide. The linear guide moved at steps of $20\mu m$ forward (backward), causing an equivalent sensor width compression (relaxation). The resulting fluorescence signal variation was transmitted by the angled tip optical fiber to the imaging system and then detected by the camera.
For each position, the force applied on the sensor was recorded by the calibration force sensor while an image was acquired by the camera. The region of interest (ROI),

corresponding to the tip of the fiber, was detected by an image processing algorithm. The intensity values associated with the pixels included in the ROI were considered to calculate the average intensity at each fiber tip.

A. Calibration

To obtain the calibration curve, the silicone pad was compressed and relaxed in the same position for thirty times. A probe of $3mm$ of diameter was used for the compression. Figure 3a is a plot of the acquired pressure readings versus the recorded average intensity. The sensor compression increment was about $130\mu m$ for each point. Force data were later converted to pressures to be comparable with typical values measured during colonoscopy as reported in literature. Data regarding maximum intraluminal pressure during routine colonoscopy range between 4 and $20kPa$, while bursting pressures have values from about $7kPa$ in the cecum to $30kPa$ in the sigmoid colon [29].
As shown by the calibration curve (fig. 3a), the presented sensor is able to measure pressures in the range of interest for this specific application. Moreover, as expected, an increase of pressure applied on the sensor corresponds to an increase of fluorescence intensity. Data are characterized by a linear correlation with R^2=0.986. The error bars represent the standard deviation, equal to 3% of the fluorescence signal readings at a specific pressure value.

B. Photobleaching

When excited, fluorescent dyes face a constant and progressive decay that eventually, with time, makes them unable to further fluoresce. Such phenomenon is called photobleaching [30] and represents one of the major limitation to the sensor life time. To measure the fluorescence signal decay caused by photobleaching, the sensor has been continuosly exposed to excitation light for 8 hours, sampling the fluorescence signal every second. The resulting data are shown in fig 3b.
It is possible to observe that after two hours the photobleaching causes an intensity decrease lower than 1%.
Considering that the mean duration of endoscopic interventions is around 30 minutes [31], photobleaching can be neglected.
The photobleaching experiment was prolonged for a further 24 hours. After that, the experiment was interrupted for one hour and resumed for another hour. The decrease of the intensity can be considered constant along time and it is not sensibly affected by interruptions of the sensor operations.
The experiment was also repeated keeping the sensor compressed by a constant force of about $15N$ for eight hours. In this case the light intensity seems to decrease slightly faster. However the slope of the signal intensity decay remains linear and of the same order of magnitude.

V. EXTENSION TO A SOFT TACTILE ARRAY SENSOR

The design shown in fig. 1d was developed to demonstrate the feasibility of a soft tactile array sensor exploiting fluorescence. The array pad presents the same layers structure as the single fiber prototype, but aims to provide the coordinates of the application point of the pressure over the sensor area. In this case, a bundle of four fibers was used. These fibers present similar diameter and same optical properties (refractive indices and materials of core and cladding) than the fibre used in section IV. Thus, the calibration curve (fig. 3a) obtained for the single fiber sensor is assumed valid with good approximation for each fibre of the array sensor. The four fibers were embedded into the flexible pad at the distance of $7mm$ between each other, going to design a square.
The five graphs in fig. 4 are a graphical representation of the sensor when a pressure is applied on five different locations. An image processing algorithm was developed to calculate the light intensity of each fiber of the bundle. Then, the application point of the pressure on the sensor was considered corresponding to the center of mass calculated as follows:

$$x_{\text{CM}} = \frac{\sum_{i=1}^{4}(x_{\text{i}} f_{\text{i}})}{\sum_{i=1}^{4} f_{\text{i}}} \qquad y_{\text{CM}} = \frac{\sum_{i=1}^{4}(y_{\text{i}} f_{\text{i}})}{\sum_{i=1}^{4} f_{\text{i}}}$$

where x_{i} and y_{i} are the coordinates of the center of each fiber tip and f_{i} is the corresponding average intensity defined as in the single fiber case. The values x_{i} and y_{i} were calculated on the basis of the geometry pattern shown in fig. 4 which is a scheme of the real position of the fibers inside the sensor array.
In all the four cases of pressure applied in correspondence of one fiber tip, the measured location falls within the blue circle representing the pressure application probe. When the middle of the sensor is pressed, the calculated position is slightly outside of the blue circle.
It should be noted that a correct detection of the position requires at least 3 fibers surrounding the application point of the pressure. Thus, due to its specific design, the sensing area of the proposed sensor corresponds to the square defined by the four fiber tips. Considering the highest uncertainty experimentally obtained (fig. 4b), it can be concluded that the proposed sensor is able to detect the application point of the pressure with an error lower than 10% of the sensing area.
Regarding the potential application of this sensor, a further design improvement is required to create a flexible covering skin for the external surface of medical tool shafts. The increase of both the flexible pad surface and the number of sensing elements, in addition to a non-planar geometry, will lead to an extension of the sensing area. In fact, more fibers would be surrounded by other fibers and it will be possible to define the application point of a pressure on a more extended surface.

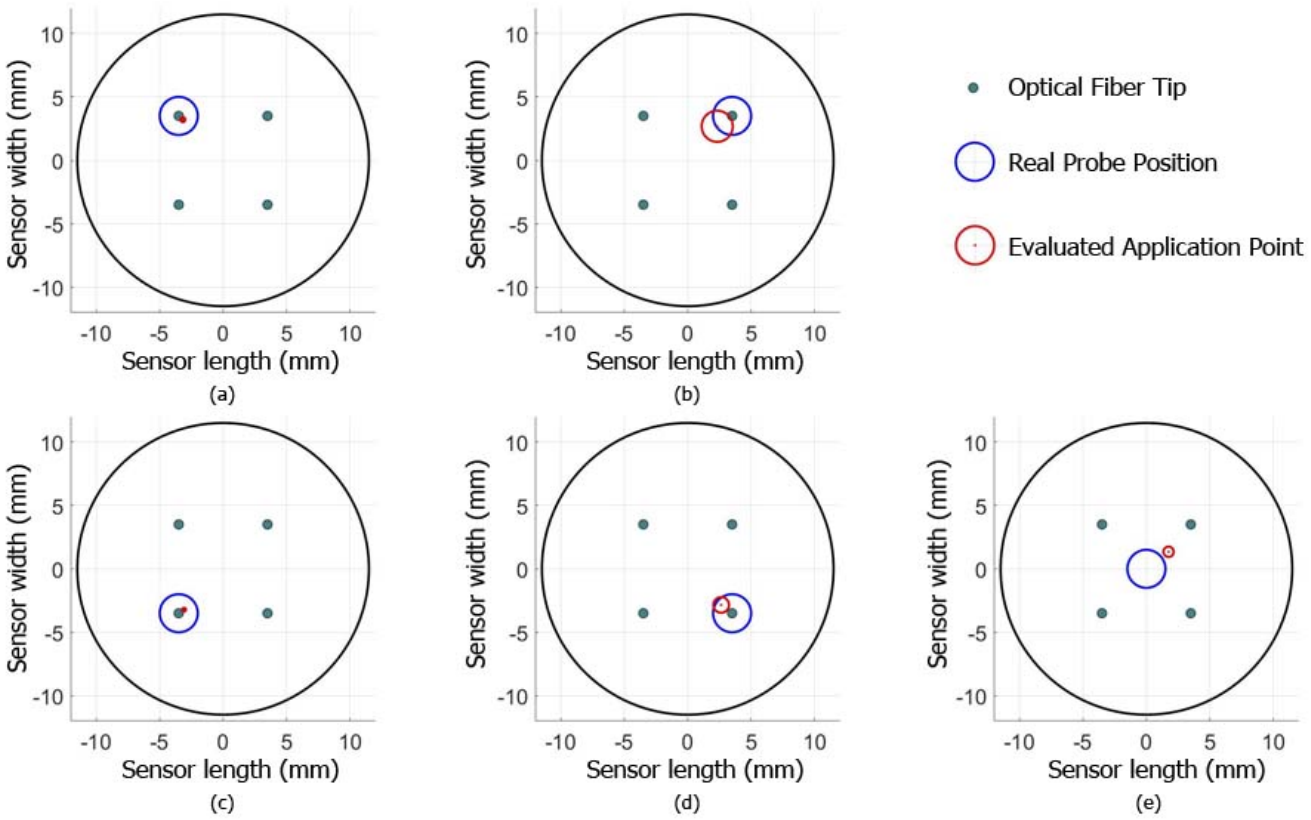

Fig. 4: **Measurement of the application point of the pressure on the sensor.** A pressure was applied on five different locations of the flexible array sensor: on the tip of each of the four fibers (grey circles) and at the center of the sensor. The sensor was pressed 10 times for each location, using a probe with a diameter of $3mm$. The blue circles represent the real position of the probe. An algorithm calculates the centre of mass on the basis of the intensity of the four fibers to evaluate the point of the pressure application (red dot). The error is the standard deviation of the repeated measurements and corresponds to the radius of the red circles.

VI. CONCLUSION AND FUTURE WORK

The introduction of fluorescence for the development of force sensors present various advantages. Fluorescence offers the possibility to distinguish between excitation and emission light on the basis of the different wavelengths. This characteristic plays a fundamental role in improving the signal-to-noise ratio. By using fluorescence in combination with an angled optical fiber tip there is no need to deploy mirrors or other rigid components favoring the flexibility of the structure. Moreover, the same optical fiber can be used both as emitter and receiver allowing further design miniaturization.

In this paper we have demonstrated how fluorescence can be successfully used to implement both single and multi-fiber array force sensors. The single fiber sensor is able to detect pressures with a repeatability of 3%. The development of a multi-fiber array sensor allowed to measure the application point of the pressure with an uncertainty lower than 10% of the sensing area. The unwanted effect of photobleaching is negligible considering the limited duration of endoscopic interventions. The relatively simple manufacturing process and its low cost can make this sensor disposable. Finally, this sensor is immune to electromagnetic interference, making it MRI compatible.

In order to apply the proposed sensor to the external surface of an endoscope shaft, shape and dimensions should be further improved and miniaturized, enabling a design with a higher density of tactile elements. It should be mentioned that the increase of number of fibers leads to significant practical challenges. For this reason, the proposed array sensor presents just four sensing elements. However, the results presented in fig. 4 show that the contact location can be identified with relatively small margin of error using the proposed method. Thus, the feasibility of the practical use of this sensor for flexible endoscopes is demonstrated.

Future works will involve the improvement of the manufacturing process for the multi-fiber array sensor. Furthermore, a comprehensive study of contact location estimation will be carried out to allow the measurement of magnitude and position of an applied pressure.

An extended design presenting a higher number of sensing elements could fit various MIS applications and it could be particularly interesting to monitor pressures applied on the external surface of a catheter during endoscopic interventions.

REFERENCES

[1] Cheng Chi, Xuguang Sun, Ning Xue, Tong Li, and Chang Liu. *Recent Progress in Technologies for Tactile Sensors.* Sensors 2018. Vol. 18, No. 4, pp. 948-977, 2018.

[2] Lona Vyas, D. Aquino, Chin-Hsing Kuo, Jian S. Dai, Prokar Dasgupta. *Flexible Robotics.* BJU Int. 2011. Vol. 107, No. 2, pp. 187–189, 2011.

[3] Hui Xie, Hongbin Liu, Yohan Noh, Jianmin Li, Shuxin Wang, Kaspar Althoefer. *A Fiber-Optics-Based Body Contact Sensor for a Flexible Manipulator.* IEEE Sensors Journal. Vol. 15, No. 6, 2015, pp. 3543-3550.

[4] Junghwan Back, Prokar Dasgupta, Lakmal Seneviratne, Kaspar Althoefer, Hongbin Liu. *Feasibility Study-Novel Optical Soft Tactile Array Sensing for Minimally Invasive Surgery.* 2015 IEEE/RSJ International Conference on Intelligent Robots and Systems (IROS). 2015, pp. 1528-1533.

[5] Liu Da, Dapeng Zhang, and Tianmiao Wang. *Overview of the Vascular Interventional Robot.* International Journal of Medical Robotics and Computer Assisted Surgery. Vol. 4, No. 4, 2008, pp. 289-294.

[6] Zhanat Kappassov, Juan-Antonio Corrales, and Véronique Perdereau. *Tactile sensing in dexterous robot hands — Review.* Robotics and Autonomous Systems. Vol. 74, Part A, 2015, pp. 195-220.

[7] Hanna Yousef, Mehdi Boukallel, and Kaspar Althoefer. *Tactile sensing for dexterous in-hand manipulation in robotics — A review.* Sensors and Actuators A: Physical. Vol. 167, No. 2, 2011, pp. 171-187.

[8] Ravinder S. Dahiya, Giorgio Metta, Maurizio Valle, and Giulio Sandini. *Tactile Sensing — From Humans to Humanoids.* IEEE Transactions on Robotics. Vol. 26, No. 1, 2010, pp. 1-20.

[9] Pinyo Puangmali, Kaspar Althoefer, Lakmal D. Seneviratne, Declan Murphy, and Prokar Dasgupta. *State-of-the-Art in Force and Tactile Sensing for Minimally Invasive Surgery* IEEE Sensors Journal. Vol. 8, No. 4, 2008, pp. 371- 381.

[10] Hiroyuki Nakamoto, Masanori Goka, Satoru Takenawa, and Yasuaki Kida. *Development of tactile sensor using magnetic elements.* In Proceedings of the IEEE Workshop Robotic Intelligence Informationally structured Space. 2011; pp. 37–42.

[11] Sunjong Oh, Youngdo Jung, Seonggi Kim, SungJoon Kim, Xinghao Hu, Hyuneui Lim, and CheolGi Kim. *Remote tactile sensing system integrated with magnetic synapse. Scientific Reports.* Vol. 7, 2017, pp. 16963–16970.

[12] Takumi Kawasetsu, Takato Horii, Hisashi Ishihara, and Minoru Asada. *Mexican-hat-like response in a flexible tactile sensor using a magnetorheological elastomer.* Sensors. Vol. 18, No. 2, 2018, pp. 587-603.

[13] Wang, H.; de Boer, G.; Kow, J.; Alazmani, A.; Ghajari, M.; Hewson, R.; Culmer, P. *Design methodology for magnetic field-based soft tri-axis tactile sensors.* Sensors. Vol. 16, No. 9, 2016, pp. 1356-1376.

[14] Hongbin Liu, Jichun Li, Xiaojing Song, Lakmal D. Seneviratne, and Kaspar Althoefer. *Rolling Indentation Probe for Tissue Abnormality Identification during Minimally Invasive Surgery.* IEEE Transactions on Robotics. Vol. 27, No. 3, 2011, pp. 450-460.

[15] M. Ohka, H. Kobayashi, and Y. Mitsuya. *Sensing characteristics of an optical three-axis tactile sensor mounted on a multi-fingered robotic hand.* 2005 IEEE/RSJ International Conference on Intelligent Robots and Systems. 2005, pp. 111-136.

[16] Pencilla Lang. *Optical Tactile Sensors for Medical Palpation.* Canada-Wide Science Fair, St. John's, NL, Canada, 2004.

[17] Panagiotis Polygerinos, Asghar Ataollahi, Tobias Schaeffter, Reza Razavi, Lakmal D. Seneviratne, and Kaspar Althoefer. *MRI-Compatible Intensity-Modulated Force Sensor for Cardiac Catheterization Procedures.* IEEE transactions on bio-medical engineering. Vol. 58, No. 3, 2011, pp. 721-726.

[18] Riadh A. Kadhim. *Strain measurement by using phase modulated fiber optics sensors technology.* Diyala Journal of Engineering Sciences. Vol. 08, No. 01, 2015, pp. 27-41.

[19] J. David Zook, William R. Herb, C.J Bassett, Terry Stark, Jeff N. Schoess, and Mark L. Wilson. *Fiber-optic vibration sensor based on frequency modulation of light-excited oscillators.* Sensors and Actuators A Physical. Vol. 83, Issues 1–3, 2000, pp. 270-276.

[20] R. E. Saad, A. Bonen, K. C. Smith, and B. Benhabib. *Distributed-force recovery for a planar photoelastic tactile sensor.* IEEE Transactions on Instrumentation and Measurement. Vol. 45, Issue 2, 1996, 541-546.

[21] Hisham Kadhum Hisham. *Optical Fiber Sensing Technology: Basics, Classifications and Applications.* American Journal of Remote Sensing. Vol. 6, No. 1, 2018, pp. 1-5.

[22] Asghar Ataollahi, Panagiotis Polygerinos, Pinyo Puangmali, Lakmal D. Seneviratne, and Kaspar Althoefer. *Tactile Sensor Array Using Prismatic-Tip Optical Fibers for Dexterous Robotic Hands.* 2010 IEEE/RSJ International Conference on Intelligent Robots and Systems. 2010, pp. 910-915.

[23] Asghar Ataollahi, Arash Soleiman Fallah, Lakmal D. Seneviratne, Prokar Dasgupta, and Kaspar Althoefer. *Novel Force Sensing Approach EmployingPrismatic-Tip Optical Fiber Inside an Orthoplanar Spring Structure.* 2014 IEEE/ASME Transactions on Mechatronics. Vol. 19, No. 1, 2014, pp. 121-130.

[24] Hui Xie, Hongbin Liu, Lakmal D. Seneviratne, and Kaspar Althoefer. *An Optical Tactile Array Probe Head for Tissue Palpation During Minimally Invasive Surgery.* IEEE Sensors Journal. Vol. 14, No. 9, 2014, pp. 3283-3291.

[25] OpenStax University Physics - All Volumes. Derived from University Physics by OpenStax University Physics. [online] *https://cnx.org/contents/pZH6GMP0@1.39:ndvbjZv5@2/Total-Internal-Reflection.* Accessed 01 March 2020.

[26] Philip Yip (2016). *Nanometrology using Time-Resolved Fluorescence*. (Doctoral dissertation). University of Strathclyde, Glasgow, Scotland.

[27] Joseph R. Lakowicz. *Introduction to Fluorescence.* Lakowicz J.R. (eds) Principles of Fluorescence Spectroscopy. Springer, Boston, MA, 2006.

[28] Fred Rost. *Fluorescence Microscopy, Applications.* In Encyclopedia of Spectroscopy and Spectrometry, Third Edition, Elsevier Ltd, Ashfield, New South Wales, Australia, 2017, pp. 565-570.

[29] R.A. Kozarek, D.L. Earnest, M.E. Silverstein, R.G. Smith. *Air-pressure-induced colon injury during diagnostic colonoscopy.* Gastroenterology. Vol. 78, Issue 1, 1980, pp. 7–14.

[30] Nathalie B. Vicente, Javier E. Diaz Zamboni, Javier F. Adur, Enrique V. Paravani, and Víctor H. Casco. *Photobleaching correction in fluorescence microscopy images.* Journal of Physics: Conference Series. Vol. 90, Issue 1, 2007, pp. 12068-12075.

[31] Dennis Yang, Robert Summerlee, Alejandro L. Suarez, Yaseen Perbtani, J. Blair Williamson, Charles W. Shrode, Anand R. Gupte, Shailendra S. Chauhan, Peter V. Draganov, Chris E. Forsmark, and Mihir S. Wagh. *Evaluation of interventional endoscopy unit efficiency metrics at a tertiary academic medical center.* Endoscopy International Open. Vol. 04, No. 2, 2016, pp. E143–E148.